Department of Defense
Legacy Resource Management Program

15-800

MEETING CONSERVATION AND COMPLIANCE NEEDS THROUGH IMPROVED GREATER SAGE-GROUSE LEK LINE-OF-SIGHT VISIBILITY ANALYSIS USING HIGHEST-HIT LiDAR DATA

Jena Ferrarese
Center for Environmental Management of Military Lands
Colorado State University
Final Report

March 2018

Department of Defense Legacy Resource Management Program

Meeting Conservation and Compliance Needs Through Improved Greater Sage-grouse Lek Line-of-Sight Visibility Analysis Using Highest-Hit LiDAR Data

Project Number 15-800

Cooperative Agreement Number HQ0034-15-2-0009

Jena Ferrarese

Center for Environmental Management of Military Lands

Colorado State University, Fort Collins, CO

CONTENTS

FIGURES

TABLES

EXECUTIVE SUMMARY

Protections for greater sage-grouse (*Centrocercus urophasianus*) on Department of Defense (DoD) lands have led to natural resources-related encroachment on military training areas. This study's primary military mission benefit is a demonstration of how developable area can be enlarged without negatively impacting sage-grouse habitat through increased visibility. This supports the military's ability to operate in areas within and adjacent to sage-grouse habitat.

This study, funded as project number 15-800 through the DoD Legacy Program Cooperative Agreement number HQ0034-15-2-0009, investigated the impacts of calculating visibility between sage-grouse breeding grounds and simulated structures across simulated landscapes that either included vegetation or were simply the ground itself.

Sage-grouse breeding success is sensitive to visibility of their breeding grounds, known as 'leks', from structures where predatory raptors may perch. In analyses of how new structures may visually impact leks, visibility is typically determined by first modeling a computerized representation of a vegetation-free landscape (a bare-earth digital elevation model [DEM]). Then, locations of straight-line, unobstructed visibility (lines-of-sight) between the lek and the potential development are calculated across that landscape. This process does not account for the obscuration of the lek by the vegetation. However, vegetation height, size and location can be accurately measured and incorporated into the model using a laser scanning technique known as light detection and ranging (LiDAR). Incorporating vegetation obstructions into modeled lines-of-sight between leks and potential development was expected to better characterize visibility, and potentially increase usable area while maintaining sage-grouse habitat quality.

The objectives of this study were to determine the impact on visibility in sage-grouse habitat from 1) varying DEM type between bare-earth and highest-hit; 2) varying simulated development structure height among 2 m, 15 m, and 50 m; and 3) varying LiDAR data density between 11.73 points/m^2 and 4.31 points/m^2. The hypotheses were that 1) points viewed across DEMs that include vegetation and other above-ground obstructions (highest-hit DEMs) would be less visible than points at the same locations viewed across bare-earth DEMs 2) shorter structures would be less visible than taller ones; and 3) points viewed across DEMs derived from higher density LiDAR data would be less visible than points at the same locations viewed across DEMs derived from lower density LiDAR data, due to more accurate obstruction (shrub) modelling.

This study's primary mission benefit is a demonstration of how finer resolution data analyses can enlarge developable area without negatively impacting sage-grouse habitat through increased visibility. This has potential to reduce natural-resources-related encroachment, as well as other types of visibility-related conflicts on training and testing areas.

FINDINGS

- Though challenging to implement, this study suggests that on suitable sites, areas excluded from development of new structures can be reduced 20 – 50% by calculating line-of-sight visibility using a highest-hit instead of a bare-earth DEM. This could allow placement of fences, power poles, towers, or other mission-related structures in areas previously thought unacceptable.
- Visibility between leks and simulated structures was lowest across topography at sites that were flat or varied, and highest at the site with fairly continuous upslope relief.
- Mean site vegetation height was not directly related to visibility between leks and simulated structures; how vegetation interacted with other scenario factors was more important. For example, visibility at the site with the shortest mean vegetation height was reduced the most when averaged across all structure heights.
- Using a highest-hit DEM instead of a bare-earth DEM reduced visibility between leks and simulated structures in all cases, although reductions ranged from 0.1 – 47.1% based on other site characteristics. Non-trivial reductions occurred in 5 of the 9 scenarios, with 23.0 – 47.1% fewer potential structure locations visible from the lek when viewed across a highest-hit DEM instead of a bare-earth DEM.
- Shorter structures were less visible from leks in every case tested. 15 m structures were visible at 21.0 – 54.0% fewer points than 50 m structures; 2 m structures were visible at 52.5 – 79.2% fewer points than 50 m structures.
- Non-trivial structure visibility reductions occurred in both data density scenarios, although the reductions from using a highest-hit DEM instead of a bare-earth DEM were a mean 50% greater when using the higher density data instead of the lower density data. This is likely because denser data better captures vegetation structure and more accurately models obstructions.
- This approach is also applicable to other species' habitat where visibility is a concern, as well as non-habitat applications, for example neighboring property owners.

RECOMMENDATIONS

Based on this study's criteria and results, using a highest-hit DEM instead of a bare-earth DEM is most likely to reduce visibility and increase land available for military activities under the following conditions:

- Sites with flat or broken topography
- Planned structures of $\leq$ 15 m
- LiDAR data density of $\geq$ 4 points/m^2, although denser data is likely more effective

1. INTRODUCTION

Across the western United States, successful management of greater sage-grouse (*Centrocercus urophasianus*) on Department of Defense (DoD) lands involves balancing habitat protection and competing, human-centered land uses.

Many anthropogenic factors have been shown to be negatively associated with sage-grouse success, including proximity to human infrastructure. Specifically, usage rates of greater sage-grouse leks have shown declines related to anthropogenic structural development, in part due to predatory raptors perching on those structures (Braun et al. 2002, Hovick et al. 2014, Walker et al. 2007). Leks are areas where male sage-grouse gather to display for females during breeding season (Figure 1), and are crucial components of sage-grouse habitat. They tend to be more open and have fewer shrubs than adjacent habitat (Connelly et al. 2004).

Figure 1. Typical sage-grouse lek. Photo credit: http://www.backcountry-utah.com/events/March%2021-2005.htm

Currently, a variety of buffer distances and line-of-sight restrictions have been proposed and/or implemented to mitigate negative impacts associated with development proximity. However, buffer distances are not guaranteed to eliminate anthropogenic structure visibility, and line-of-sight restrictions vary among regulations. Examples of line-of-sight restrictions include the Idaho Natural Resources Conservation Service recommendation to "avoid grazing within the lesser of 0.6mi or direct line-of-sight of occupied leks … (*Greater Sage-Grouse Habitat Conservation Strategy* n.d.)," the Bureau of Land Management instruction that "The siting of new temporary MET towers must be avoided within 2 miles of active sage-grouse leks, unless they are out of the direct line-of-sight of the lek (Roberson 2009)," and the constraint on the Keystone XL pipeline construction from March 1 through June 15 around active sage-grouse leks if "The Project is within 3 miles of a lek and within the line-of-sight of the lek (Farmer and Beaver 2010)."

Although line-of-sight is used as a suggested restriction, the above examples do not specify how that line-of-sight should be assessed. One currently-employed approach to modeling line-of-sight is to use viewshed analysis of a bare-earth digital elevation model (DEM) within a geographic information system (GIS). However, this does

not take into account the existing vegetation on a site, which has the potential to limit visibility by intercepting the line-of-sight (Figure 2).

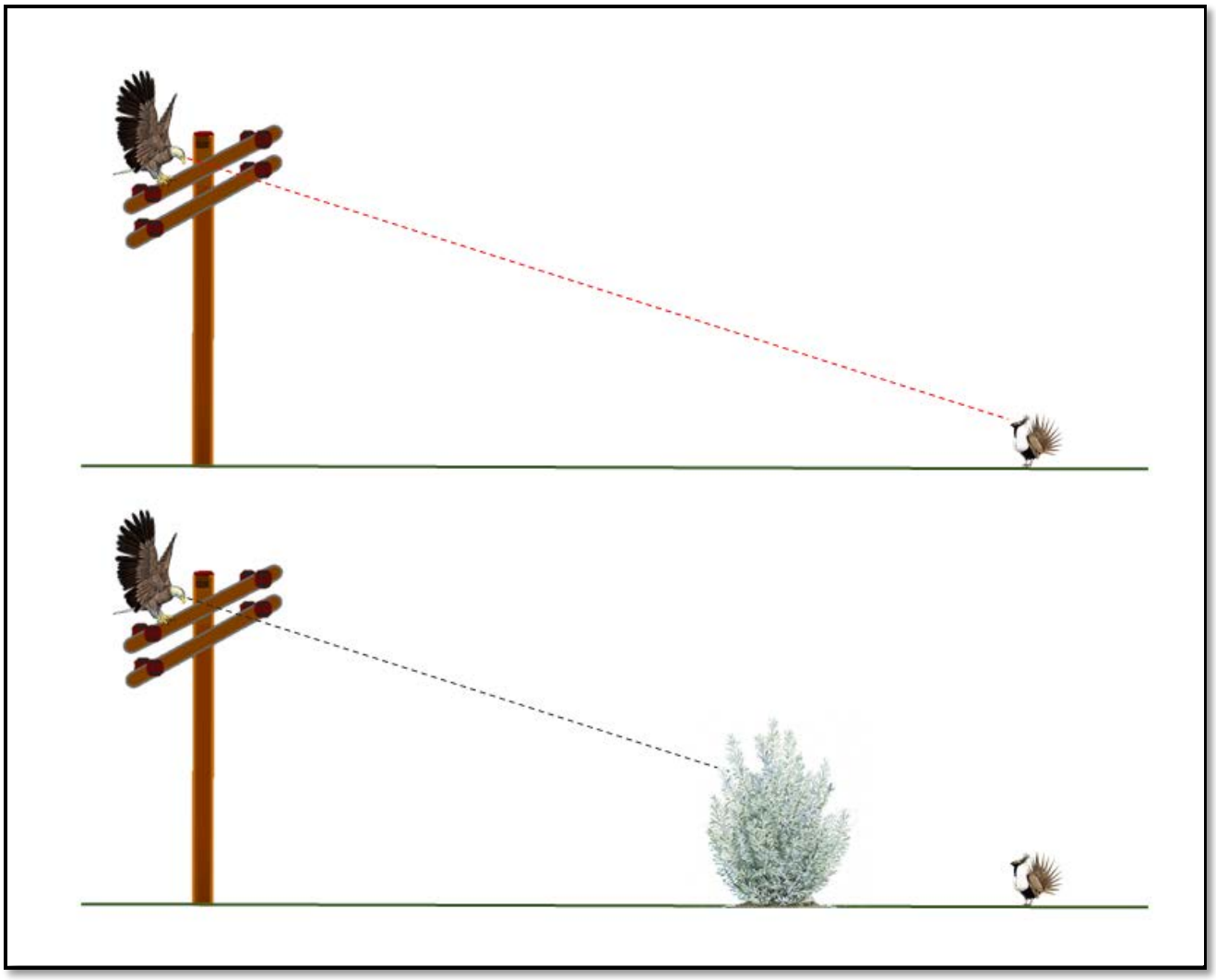

Figure 2. Line-of-sight with (bottom) and without (top) vegetation. Whereas the top panel has an unbroken line-of-sight from the sage-grouse to the raptor, in the bottom panel this is interruped by the sagebrush. Note that figure components are for visualization purposes only, and are not to scale.

Capturing the vegetation structure though use of light detection and ranging (LiDAR) data, and using DEMs built from “highest-hit” datasets instead of solely “bare-earth” data, can provide a more accurate characterization of structural visibility. Highest-hit DEMs use the highest recorded point within a cell to determine the elevation for that cell, whereas bare-earth DEMs typically use a mean of the ground point elevations within the cell. Highest-hit DEMs capture the ground as well as any vegetation or human-built objects on it, and bare-earth DEMs describe topography alone.

Although a highest-hit DEM can be created from any LiDAR dataset, point density drives DEM resolution (cell size), and coarser resolution (i.e., larger cell sizes) may not adequately represent smaller features such as shrubs.

If the shrub structure is not adequately captured, the impact on visibility may be underestimated. Vierling (2012) found automated shrub detection rates varied with DEM spatial resolution, and that 4 points/m^2 data produced shrub heights well-correlated with field measures, but not shrub crown area. Conversely, both shrub heights and crown area derived from 16 points/m^2 data were well-correlated with field measures. Intermediate within that density range, Mitchell et al. (2011) found that a LiDAR dataset of 9.46 points/m^2 successfully captured both shrub heights and canopy area in a sagebrush shrubland.

LiDAR data of this quality are becoming more common, but are not universally available. Suitable data were not available for the military installations that both have sage-grouse populations and supported this study. For example, Yakima Training Center had LiDAR data available at approximately 1.1 points/m^2, a density too low for this study. The United States Geologic Survey (USGS) has begun collecting LiDAR data over the contiguous U.S., Hawaii, and U.S. territories at their defined Quality Level (QL) 2, a point density of only 2 points/m^2. However, the USGS LiDAR guiding document (Heidemann 2014) also provides data collection specifications for QL1 and QL0, which have defined point densities of at least 8 points/m^2.

Both the Oregon LiDAR Consortium and Puget Sound LiDAR Consortium have adopted technical specifications for their public domain LiDAR data requiring pulse densities greater than or equal to 8 points/m^2 (Oregon LiDAR Consortium and Puget Sound LiDAR Consortium). Similarly, much of Massachusetts is available at the USGS QL1 level through a buy-up option executed in partnership with the USGS (MassGIS 2017). Lastly, many university LiDAR research groups make their high-quality data available, including Idaho State University whose personnel work in shrublands of the western United States.

The objective of this study were to determine the impact on visibility in sage-grouse habitat from 1) varying DEM type; 2) varying structure height; and 3) varying data density. The hypotheses were that 1) points viewed across highest-hit DEMs would be less visible than points at the same locations viewed across bare-earth DEMs, due to incorporation of above-ground obstructions; 2) shorter structures would be less visible than taller ones; and 3) points viewed across DEMs derived from higher density LiDAR data would be less visible than points at the same locations viewed across DEMs derived from lower density LiDAR data, due to more accurate obstruction (shrub) modelling. Using visibility calculated for a series of random points at each site, both the counts and the spatial distributions of points were used to assess the impact of each variable, and test each hypothesis.

This study used publicly available LiDAR data covering non-DoD rangelands in Idaho, but the results are also applicable to shrublands on DoD installations across the western United States. Increasing the developable area adjacent to sage-grouse leks without compromising habitat quality reduces natural-resources related encroachment on training activities. This study was fully funded as DoD Legacy Program Project Number 15-800, and directly supports the Legacy Program Readiness and Range Sustainment Area of Emphasis.

2. METHODS

Each of the sections below describes one aspect of this study's design and execution. Additional data is found in Appendix B – Raster Generation Parameters.

2.1 SITE SELECTION

There are 2,162 sage-grouse leks in the Idaho lek database (Idaho Sage-grouse Advisory Committee 2016); the limiting factor in site selection for this study was lek location in areas overlaid with high-density LiDAR (see 2.2). Among leks that were suitably located, sites were chosen to represent a range of topographic and vegetative characteristics. Site locations and reference names (below) are shown in Figure 3.

Sites:

- Borah Scarp, Mackay, ID – "Borah Scarp"
- Camas National Wildlife Refuge, Mud Lake, ID – "Camas NWR"
- Reynolds Creek Experimental Watershed, Murphy, ID – "Reynolds Creek"

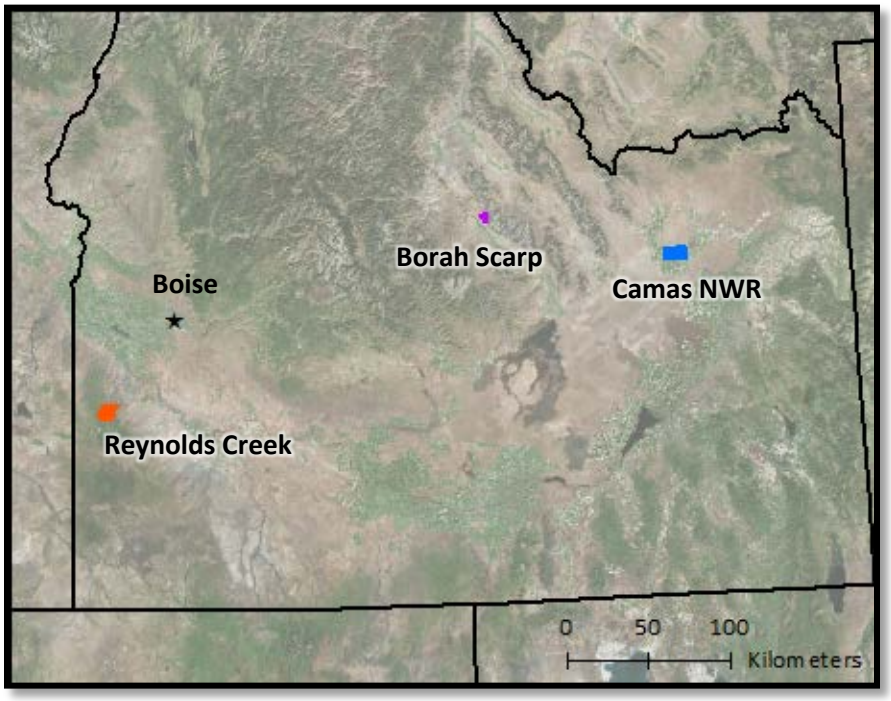

Figure 3. Site locations across southern Idaho. The Borah Scarp site is purple, Camas NWR is blue, and Reynolds Creek is orange. Boise, the state capital, is marked with a black star.

The Borah scarp site is largely a gradual west to east up-slope with gentle topography, but is backed by steeper terrain (the toe slopes of Mt. Borah) on the east side. The vegetation at the Borah scarp site is a sagebrush and grassland mix, with aspen (*Populous tremuloides*) and western juniper (*Juniperus occidentalis*) in the eastern valleys where soil moisture increases. The Camas NWR site is flat, and vegetation varies with elevation and distance from the west-central lake. The upland areas are mostly big sagebrush (*Artemesia tridentata*)-steppe. The Reynolds Creek site is a mix of steep hills and gullies, with a wider valley floor running through the center of the watershed. Reynolds Creek vegetation at lower elevations is a mix of sagebrush (Wyoming big sagebrush [*A. tridentata subsp. wyomingensis*], low sagebrush [*A. arbuscula*], and mountain big sagebrush [*A. tridentata*

subsp. vaseyana]) and grassland communities, with aspen (*P. tremuloides*) and Douglas fir (*Pseudotsuga menziesii*) common at higher elevations. Elevation and vegetation profiles for each site are in Appendix A.

Estimated lek locations were identified using publicly available documents and Google Earth, and refined through conversations with local land managers who provided detailed coordinates (Table 1).

Table 1. Initial lek coordinates used for each study site.

Site	Latitude (degrees)	Longitude (degrees)
Borah Scarp	44.160554	-113.872959
Camas NWR	43.907294	-112.346368
Reynolds Creek	43.140931	-116.745680

Although provided as point locations, a single point does not capture the actual lek usage, which would include multiple birds across a larger area. To represent this, estimated lek boundaries surrounding each initial location were developed based on vegetative characteristics observed on aerial imagery. Then, at each site, 15 random points were generated within the estimated boundary. Three of these points, spaced across the estimated lek area, were chosen and used as inputs to the visibility calculations. The points used for each lek are included as a GIS feature class within the delivered geodatabase.

2.2 LIDAR DATA ACQUISITION

Department of Defense installations that actively manage for greater sage-grouse span the western United States (e.g. Yakima Training Center, WA; Nellis Test and Training Range, NV; Mountain Home Air Force Base, ID; and others). However, those installations were not covered by LiDAR data of sufficient density for this study. Instead, publicly accessible data that met the necessary specifications was used, even though it was collected over non-DoD lands. This data was suitable for a proof-of-concept project.

The data used in this study were provided at no cost through the Idaho LiDAR Consortium website (http://www.idaholidar.org/data). The datasets chosen all had LiDAR point data available, a reported data density of at least 9 points/m^2, and covered areas identified as Priority, Important, and/or General Habitat in the *Greater Sage-Grouse Habitat Management Areas of the Great Basin Region, Idaho-SW Montana Sub-region, Greater Sage-grouse Environmental Impact Statement (EIS) - Administrative Draft Proposed Plan, as updated for inclusion of Sagebrush Focal Areas* (U.S. Department of the Interior 2015). The LiDAR data from each site were collected as independent projects, not connected to this study or to each other.

2.3 LIDAR DATA PRE-PROCESSING AND ELEVATION MODEL GENERATION

Both the Borah Scarp and Camas NWR LiDAR points had been classified by the data vendor into ground and non-ground classes. Visual inspection of those classes showed acceptable classifications, and no need for additional editing before generating digital elevation models (DEMs). Each dataset was input into an ArcGIS 10.2 (ESRI 2013) .LAS dataset, and converted to rasters using standard ArcGIS tools. At each site, ground points were used to generate a bare-earth DEM, and all valid points (i.e., excepting those classed as noise) were used to create a highest-hit DEM. For this study, the highest-hit raster was generated using all points not classified as noise, and

should not be considered solely a vegetation raster. For example, the Camas NWR dataset included returns from buildings located within the coverage area. See Appendix B for settings and parameters used to create each raster.

The Reynolds Creek dataset was unclassified, and required class assignment before DEM generation. This was done using the Boise State Aerospace Laboratory (BCAL) Lidar Tools (n.d.), which provide an integrated workflow from start to finish. Raw points were buffered and height filtered following Streutker and Glenn (2006). The resulting classified data were used to generate bare-earth rasters, which were mosaicked into a final bare-earth raster covering the full study site. See Appendix B for settings and parameters used in each step.

The Borah Scarp dataset was used in its entirety – all of the LiDAR files were used to create the rasters that were used for the visibility analysis. The total study area was 15.28 km^2. The original Camas NWR and Reynolds Creek datasets were quite large; the area of analysis was limited to 103.51 km^2 for Camas NWR and 76.89 km^2 for Reynolds Creek.

Figure 4 shows multiple views of a sample area of Camas NWR: aerial imagery (A), highest-hit DEM (B), and bare-earth DEM (C). The lower panel (D) shows a cross-section of the LiDAR points, located at the A – A' transect shown on each panel. All the points were used to build the highest-hit DEM, whereas only the ground-classified points (those shown in orange in panel D) were used for the bare-earth DEM. The individual shrub on the left end of the transect is clearly visible in the LiDAR data, as is the shrub group on the right, and the slight hillslope crossed by the transect.

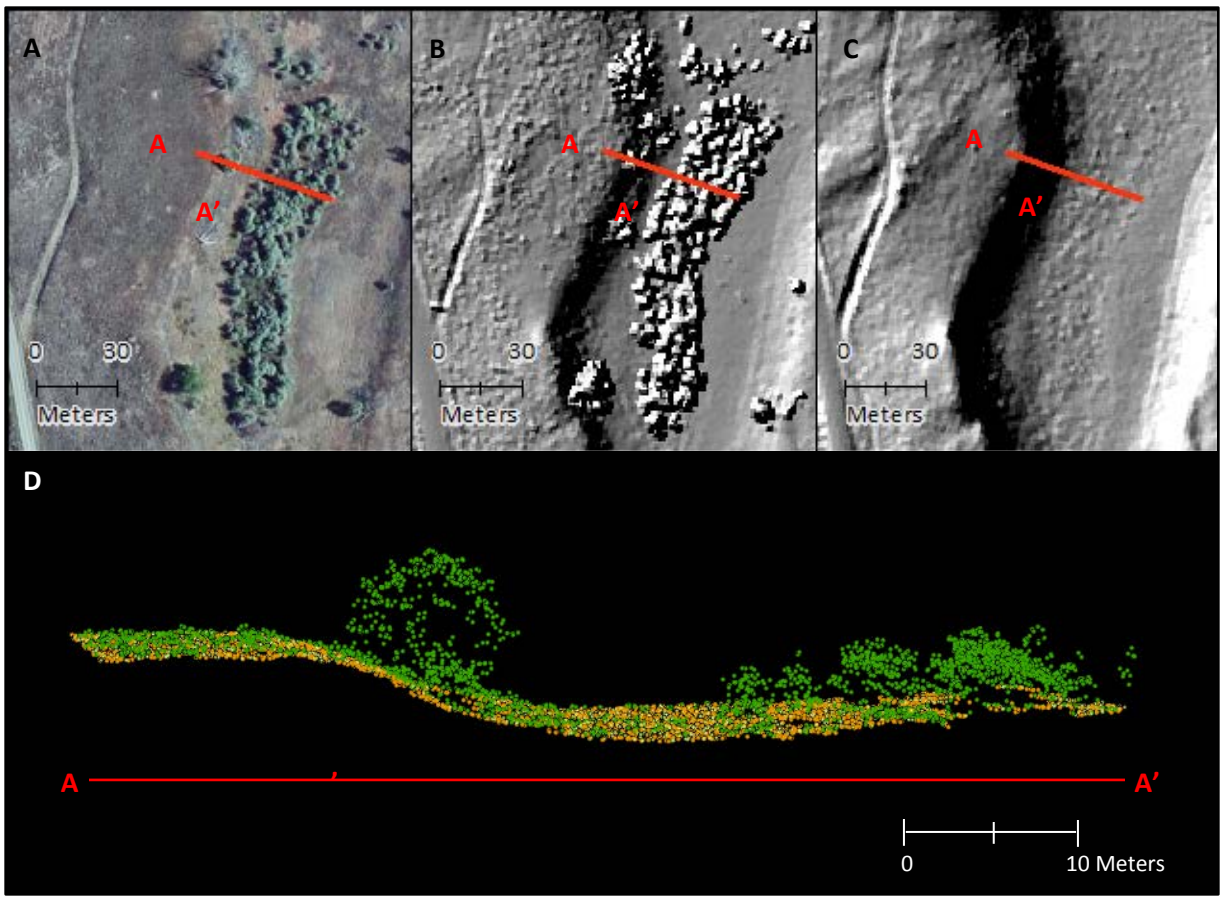

Figure 4. Left to right: (A) aerial imagery, corresponding (B) highest-hit and (C) bare-earth digital elevation model (DEM) hillshades for one area of the Camas National Wildlife Refuge (NWR) site. Note the two-track road visible in the left side of all 3 images. LiDAR data cross-section (A-A') is shown below (D). In the LiDAR cross-section, orange points are classified as ground, and green as non-ground.

To investigate the effects of data density on visibility calculation, the Camas NWR dataset was reduced from a mean point density over non-water areas of 11.73 points/m^2 (0.29 m mean point spacing) to 4.31 points/m^2 (0.48 m mean point spacing) using the Decimate LAS Files tool in the BCAL LiDAR Tools (n.d.). After decimation, bare-earth and highest-hit DEMs were generated using ground points or all valid points (i.e., excepting those classed as noise), respectively.

2.4 VISIBILITY ANALYSIS

For this study, 3 structures of varying heights were simulated, representing fences (2 m), telephone or electrical poles (15 m), and communication towers (50 m).

Within each study area, 100,000 random points, spaced at least 5 m apart, were generated, replicated to 3 datasets, and assigned heights of 2 m, 15 m, or 50 m. All the points in a random point dataset replicate were assigned the same height. Visibility was calculated across bare-earth and highest-hit DEMs, from each of 3 lek points to each of the random points, for a total of 1,800,000 visibility calculations at each site. Figure 5 shows the scenarios for one lek point at one study site. For each random point, the visibility from the 3 lek points was consolidated, so that if the random point was visible from any of the 3 points, it was considered visible from the

lek. The final data set was a binary visibility assessments (0: not visible, 1: visible) for each of 100,000 points in 6 scenarios (3 structure heights on each of a bare-earth or highest-hit DEM).

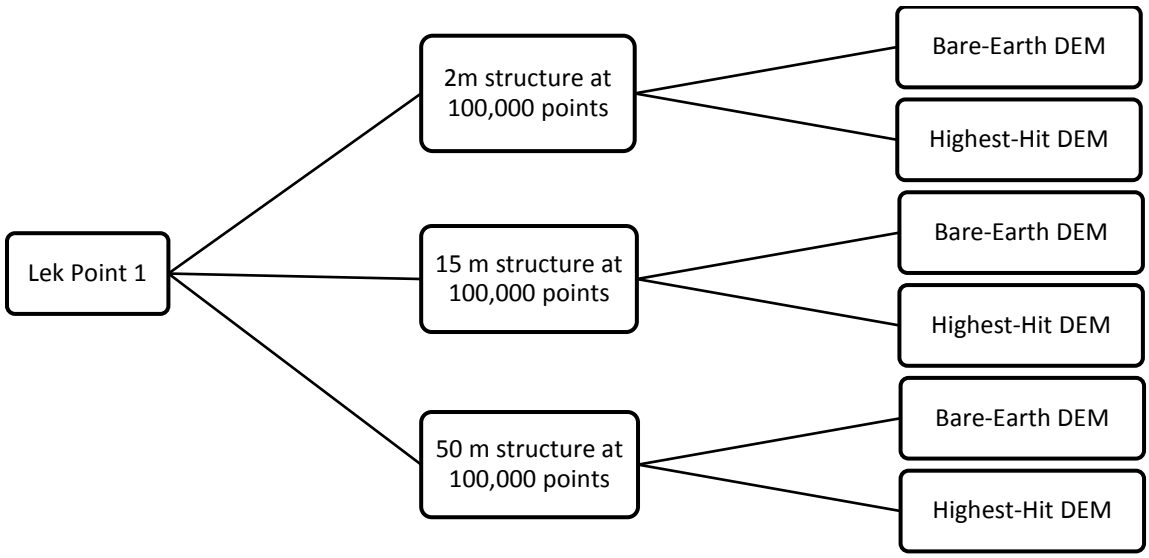

Figure 5. Visibility scenarios for one lek point at one study site, comprised of 3 structure heights applied to 100,000 random points, across each of two DEM types. At each study site, 3 lek points were used, for a total of 1,800,000 visibility calculations at each of 3 sites. Individual results from the 3 lek points were consolidated to a binary visible/not visible for each scenario (structure height and DEM).

The ArcGIS 10.2 Visibility tool was used to calculate preliminary bare-earth viewshed rasters. For each structure height at each site, the Visibility tool iterated over each of the 3 lek points. For each lek point, the chosen structure was simulated sequentially in every cell of the bare-earth raster, and, for each cell, was determined to be visible or hidden from the lek point, based on line-of-sight over the intervening topography. Cells that were located in water bodies were included, and the water was treated as any other open, flat surface. The lek points were elevated by 0.5 m, to simulate the perspective of a sage-grouse. Each cell was attributed with a count of the number of lek points visible from it (count range of 0-3). Nine viewsheds were initially calculated (3 structures on a bare-earth DEM for each of 3 sites), and 3 additional viewsheds were subsequently calculated after data decimation at one site (see Section 0). The raster values for each viewshed were extracted to the random points for that study site, and any value greater than 0 (i.e., visible from one or more lek points) was converted to 1.

Highest-hit visibility was calculated using the ArcGIS 10.2 3D Visibility tools. First, sightlines were calculated between the 3 lek points elevated 0.5 above the surface and each of the random points elevated to each of the structure heights. Using the Intervisibility tool, each sightline was intersected with the highest-hit DEM for the study area. If a sightline did intersect the DEM, the view was assumed to be blocked, and the random point was considered not visible from that lek point. If a sightline did not intersect the DEM, the view was considered uninterrupted and the random point was considered visible from that lek point. The visibility for each random point was determined based on the combined visibility from all 3 lek points; if the random point was visible from any of the lek points it was considered visible from the lek.

2.5 SHAPE METRICS CALCULATION

For each of eighteen scenarios (each structure on each DEM at each site), a two standard deviation ellipse was created using the Directional Distribution tool in ArcGIS 10.2 to capture the spatial dispersion of the visible points. A two standard deviation ellipse should encompass approximately 95% of the input point set. The ellipse width and length parameters were the two standard deviation values of the x- and y-coordinates, respectively, of the visible point set. The ellipse parameters were compared among scenarios to quantify spatial differences in visibility extent.

3. RESULTS AND INTERPRETATION

In order to examine the impact of using a highest-hit vs. a bare-earth DEM, this study relied on two measures. The first, and most important, was the count of visible points in each scenario. These results are presented as a series of comparisons that each isolate one variable (e.g. site, DEM type, structure height, etc.) in Section 3.1. The second metric was the landscape extent of the visible points, as measured by a two standard deviation ellipse. These results are presented in Section 3.2 and Appendix C – Shape Metric Additional Results. Data density variation results are found within each section.

3.1 VISIBILITY COUNTS

Because there are multiple variables among scenarios, multiple analyses were required to isolate each variable. DEM type had 2 variables (bare-earth and highest-hit), structure height had 3 (heights of 2, 15, and 50 m), and site had 3 (Borah Scarp, Camas NWR, and Reynolds Creek).

The first analysis related visibility variation to site differences. Topography and vegetation are both drivers of visibility, and these varied among the 3 sites. Section 3.1.1 presents visibility results in light of site characteristics. A second analysis isolated visibility variation related to DEM type, keeping structure height constant. This analysis compared the bare-earth and highest-hit DEMs for the 2 m structure separate from those of the 15 m, and both of those separate from the 50 m. Results from this type of comparison are found in Section 3.1.2. A third analysis isolated visibility variability among structure heights, on each type of DEM separately. Results from this type of comparison are found in Section 3.1.3.

Lastly, differences between the original and thinned Camas NWR datasets are presented as they relate to both DEM type and structure height. Because the original and thinned data are from the same site, site characteristics were constant. Any differences in how they were captured in each dataset reflect differences between the data densities.

Site characteristics, DEM type, structure height, and data density all impact visibility. Although these factors interact, examining them separately can provide insight into the contribution of each to the overall impact on visibility.

3.1.1 VARIATION BY SITE

The visibility reduction between bare-earth and highest-hit DEMs differed among study sites, and among structures at each site (discussed further in Sections 3.1.2 and 3.1.3). The 2 m structure had the greatest range of reductions across study areas, and serves as a good example for illustrating visibility variability due to site differences. Table 2 shows the reduction in visibility for a 2 m structure from using a highest-hit elevation model instead of a bare-earth model; reduction percentages range from 7.7% at Borah Scarp to 47.1% at Reynolds Creek. More fundamentally, the visible point counts, compared within each type of DEM, also varied widely for both the bare-earth and highest-hit DEMs (e.g. 12,459 visible points using the bare-earth DEM at Reynolds Creek to 44,202 visible points at Borah Scarp). This variability can be directly attributed to site characteristics differences.

Table 2. Differences across sites in visible point counts related to digital elevation model (DEM), as calculated through visibility analyses using a 2 m structure.

		Visible Points (count)			
Site	Structure Height (m)	Bare-Earth DEM	Highest-Hit DEM	Highest-Hit% of Bare-Earth	% Reduction using Highest-Hit
Borah Scarp	2	44202	40777	92.3	7.7
Camas NWR	2	14296	9426	65.9	34.1
Reynolds Creek	2	12459	6586	52.9	47.1

The small reduction in visibility, and highest point counts, at the Borah Scarp site are likely due to the gently sloping, fairly consistent elevation increase away from the lek. This acts like a natural amphitheater, facilitating visibility from the upper elevations to the lek below. Visibility at Borah Scarp is also the least interrupted by vegetation: the mean height difference between the highest-hit and bare-earth DEMs was 0.29 m. This height should not be considered the mean vegetation height, as it also incorporates areas of minimal or no vegetation. However, when compared to the values for the other sites (Table 3), it reflects less and/or shorter vegetation overall, both of which would lessen the impact of vegetation on visibility.

Table 3. Characteristics of each study site: mean and standard deviation difference between the highest-hit (HH) and bare-earth (BE) DEMs, in meters; elevation range across the entire bare-earth DEM.

Site	HH – BE Mean (m)	HH – BE Standard Deviation (m)	Elevation Range of Bare-Earth DEM (m)
Borah Scarp	0.29	1.33	454.59
Camas NWR	0.13	0.81	43.85
Reynolds Creek	0.99	3.02	850.69

Camas NWR had 34.1% reduction in visibility when using the highest-hit instead of the bare-earth DEM, and intermediate values for visible point counts (Table 2). Although the mean height difference between the DEMs was smallest at Camas NWR, the topography was the most level (Table 3). This demonstrates the interaction of vegetation and topography on visibility, as vegetation is most likely to intercept the line-of-sight between the lek

and a structure when that line-of-sight is at lower angles. Whereas the Borah Scarp site topography facilitated visibility, the flatness of Camas NWR (an order of magnitude less relief than both other sites) enabled a greater visibility reduction from vegetation than might be expected based solely on the small mean height difference at that site.

Reynolds Creek results also demonstrate the impacts of both vegetation and topography. The Reynolds Creek visibility reduction was the largest among the sites (47.1%), and the visible point counts were the smallest, even though the relief was also the largest. However the topographic differences between the Borah Scarp and Reynolds Creek sites are important. Unlike the relatively continuous gradient of the Borah Scarp site, the topography at Reynolds Creek is more broken, with a series of ridges and valleys included in the study site. These features both facilitated visibility (on slopes facing the lek, as at the Borah Scarp site), as well as blocked it (line-of-sight to a structure on the backside of a ridge would be blocked by the ridge itself, regardless of the vegetation). The lowest bare-earth visible point count among all the sites (Table 2) indicates the strong influence of topography independent of vegetation. Reynolds Creek also had the largest mean height difference between bare-earth and highest-hit DEMs, and this produced the greatest visibility reduction of all the sites. Less of the site was potentially visible, but in the areas that were, vegetation was a large influence on visibility.

3.1.2 VARIATION BY ELEVATION MODEL TYPE

In addition to comparing among sites, it is important to examine variability within each site, by DEM type or structure height. In this section, counts of visible points are compared between the bare-earth and highest-hit DEMs for each structure height. Isolating DEM variation gives a direct measure of visibility change due to vegetation for each structure height. Because the bare-earth visibility counts were always higher, each structure height's highest-hit visible point count is presented as a percentage of its respective bare-earth count.

Table 4 shows the visibility calculated using each DEM (bare-earth or highest-hit) for each structure height at each site. The Borah Scarp site showed modest reductions (7.7%) in the number of points visible from the lek when considering a 2m structure; little difference was seen using the taller structures (15 m or 50 m) at the Borah Scarp site. The Camas NWR data showed similar visibility reductions for all structures using the highest-hit DEM compared to the bare-earth DEM, approximately 4.7 times that of the Borah Scarp 2 m reduction percentage. Like the Borah Scarp site, Reynolds Creek reduction percentages varied by structure height, with the greatest reduction occurring with the 2 m structure. However, the Reynolds Creek 2 m reduction was over 6 times that of Borah Scarp. The visibility reduction from using the highest-hit instead of bare-earth DEM was also notable for the 15 m structure at Reynolds Creek, although the reduction percentage associated with the 50 m structure was small.

Table 4. Difference in visible point counts related to DEM, as calculated through visibility analyses.

		Visible Points (count)			
Site	Structure Height (m)	Bare-Earth DEM	Highest-Hit DEM	Highest-Hit% of Bare-Earth	% Reduction using Highest-Hit
Borah Scarp	2	44202	40777	92.3	7.7
	15	73442	72764	99.1	0.9
	50	92975	92874	99.9	0.1
Camas NWR	2	14296	9426	65.9	34.1
	15	30759	19419	63.1	36.9
	50	56544	35064	62.0	38.0
Reynolds Creek	2	12459	6586	52.9	47.1
	15	18892	14548	77.0	23.0
	50	32802	31624	96.4	3.6

At both Borah Scarp and Reynolds Creek, the greatest reduction in visibility occurred with 2 m structures, while the vegetation was the least effective at obscuring 50 m structures. However, the degree of reduction varied between the two sites, with Reynolds Creek always having a greater reduction in visibility, for any structure height. At Camas NWR, the percentage of visibility reduced actually increased slightly with taller structures, although the variation is small.

Overall, the data support accepting the first hypothesis, that points viewed across highest-hit DEMs would be less visible than points at the same locations viewed across bare-earth DEMs. However, these results do indicate that the benefit from using a highest-hit DEM varies by both structure height and site characteristics. On flatter sites, a meaningful reduction may be realized with any structure height whereas on more variable terrain, a meaningful reduction may not occur with taller (e.g., 50 m) structures.

3.1.3 VARIATION BY STRUCTURE

Within each site, comparisons among structure heights (while holding DEM type constant) are the counterpart to comparisons between DEM types, as described in the previous section. Here, counts of visible points are compared among the 3 structure heights, for each DEM type. Because the 50 m visible point counts were always greater than either the 2 or 15 m counts, each structure height's visible point count was calculated as a percentage of its respective 50 m count.

When using solely the bare-earth DEM to calculate visibility, variable results among structure heights were due to topographic impacts on visibility. If a taller structure is visible where a shorter one is not, that is because the shorter one is blocked by topography alone, not vegetation.

Table 5 shows the points visible using each type of DEM, relative to the maximum number visible from that same type of DEM. In all cases, the maximum visible count was associated with the 50m structure. Relative to the 50 m structure visibility, shorter structures at Borah Scarp were more visible than those at either Camas NWR or Reynolds Creek. However, even the scenario with the least amount of change from the 50 m structure (the Borah Scarp 15 m structure on the bare-earth DEM) had 21.0% fewer visible points. Although 3 points are

insufficient to derive a mathematical relationship between structure height and visible point count, it is clear that shorter structures were visible at fewer random point locations than their taller counterparts, regardless of DEM type or site characteristics. The results consistently support the second hypothesis, that shorter structures should be less visible than taller ones.

Comparing the visibility trends among structure heights on the bare-earth DEM and those same trends from the highest-hit DEM gets at the interaction of topography and vegetation cover. If vegetative cover were completely even and continuous, the proportion of visible points at each structure height (relative to the maximum number) would be quite similar between bare-earth and highest-hit DEMs. Disparity between bare-earth and highest-hit relative percentages reflects vegetation patchiness and height irregularity.

At both Borah Scarp and Camas NWR, the percentage of the maximum visible points at 2 m and 15 m was similar between the bare-earth and highest-hit DEM results. Conversely, Reynolds Creek 2 m and 15 m bare-earth relative percentages differed from their respective highest-hit relative percentages. Deviation of the highest-hit relative visible point percentage from the bare-earth percentage likely indicates a larger degree of spatial irregularity in the vegetation at Reynolds Creek than at Borah Scarp or Camas NWR.

Table 5. Differences in visible point counts related to structure height, as calculated through visibility analysis.

		Bare-Earth			Highest-Hit		
Site	Structure Height (m)	Count	% Max Count	% Reduction	Count	% Max Count	% Reduction
Borah Scarp	2	44202	47.5	52.5	40777	43.9	56.1
	15	73442	79.0	21.0	72764	78.3	21.7
	50	92975	100	-	92874	100	-
Camas NWR	2	14296	25.3	74.7	9426	26.9	73.1
	15	30759	54.4	45.6	19419	55.4	44.6
	50	56544	100	-	35064	100	-
Reynolds Creek	2	12459	38.0	62.0	6586	20.8	79.2
	15	18892	57.6	42.4	14548	46.0	54.0
	50	32802	100	-	31624	100	-

3.1.4 VARIATION BY DATA DENSITY

Although the LiDAR data used in the sections above were all high density datasets, that level of data quality is far from universal. LiDAR datasets with lower point density capture vegetative structure less accurately (Magnusson et al. 2007, Vierling 2012), which has potential to impact calculated lines-of-sight. Less dense data decreases the likelihood of capturing the maximum height of vegetation or other structures, which would underrepresent that structure's impact on visibility (e.g. it is easier to see over a 3 ft. shrub than a 5 ft. shrub).

To determine the impact of data density on visibility, this study compared the visibility results between the original Camas NWR datasets (11.73 points/m^2), and a copy that had been thinned to 4.31 points/m^2, a more

typical data density. Because all other factors were held constant, including the placement of random points, differences in calculated visibility can be attributed to data density variation.

First, a direct comparison was made between the count of visible points for each structure height on each type of DEM, between the original and decimated datasets (Table 6). Fewer points were visible using the original, denser, data for every structure height on both types of DEM. However, the disparity was larger when using the highest-hit DEM, suggesting that point density as a collection parameter becomes more important when anticipating using a highest-hit DEM to calculate visibility, instead of a more conventional approach using a bare-earth DEM.

Table 6. Differences in visible point counts between original and decimated datasets.

		Bare-Earth DEM		Highest-Hit DEM	
Site	Structure Height (m)	Visible Point Count	Decimated % of Original Count	Visible Point Count	Decimated % of Original Count
Camas NWR	2	14296	-	9426	-
	15	30759	-	19419	-
	50	56544	-	35064	-
Camas NWR Decimated	2	16822	117.7	12279	130.3
	15	33490	108.9	25372	130.7
	50	60918	107.7	46555	132.8

Next, visible point counts were compared between the bare-earth and highest-hit DEMs for each structure height. Because the bare-earth counts were always greater, each structure height's highest-hit visible point count is presented as a percentage of its respective bare-earth count.

Table 7 shows the variation in visibility calculated using different DEMs (bare-earth or highest-hit) for each structure height using the original Camas NWR data, and the results from using the decimated LiDAR data. Compared to the original degree of visibility reduction for any given structure height using the highest-hit DEM instead of the bare-earth DEM, the decimated data results showed smaller reductions between the two DEMs. Using the original data density produced a mean 50% greater reduction in visibility when calculated from a highest-hit instead of bare-earth DEM than using the decimated data. This suggests that although using a high-density LiDAR dataset may produce more impactful results when using a highest-hit DEM to calculate visibility, a more typical data density can still produce a highest-hit DEM that measurably decreases visibility when compared to the bare-earth DEM.

Table 7. Differences in visible point counts related to DEM type, as calculated through visibility analysis.

		Visible Points (count)			
Site	Structure Height (m)	Bare-Earth DEM	Highest-Hit DEM	Highest-Hit% of Bare-Earth	% Reduction using Highest-Hit
Camas NWR	2	14296	9426	65.9	34.1
	15	30759	19419	63.1	36.9
	50	56544	35064	62.0	38.0
Camas NWR Decimated	2	16822	12279	73.0	27.0
	15	33490	25372	75.8	24.2
	50	60918	46555	76.4	23.6

Lastly, counts of visible points were compared among the 3 structure heights, for each DEM type. Because the 50 m counts were always greatest, each structure height's visible point count was calculated as a percentage of its respective 50 m count.

Table 8 shows the percentage of points visible using each type of DEM, relative to the maximum number visible with that DEM, for both the original Camas NWR data and the decimated data. In each case, shorter structures were visible at few random point locations. As relative percentages of the visible point counts for 50 m structures, the decimated data bare-earth DEM results were quite similar to those from the original data. This indicates that the vegetation variability captured from both the original and decimated data is similar.

Table 8. Differences in visible point counts related to structure height, as calculated through visibility analysis.

		Bare-Earth DEM		Highest-Hit DEM	
Site	Structure Height (m)	Count	% Max Count	Count	% Max Count
Camas NWR	2	14296	25.3	9426	26.9
	15	30759	54.4	19419	55.4
	50	56544	100	35064	100
Camas NWR Decimated	2	16822	27.6	12279	26.4
	15	33490	55.0	25372	54.5
	50	60918	100.0	46555	100.0

The results of varying the data density support accepting the third hypothesis, that points viewed across DEMs derived from higher density LiDAR data would be less visible than points at the same locations viewed across DEMs derived from lower density LiDAR data. However, this was one comparison and may not indicate a universal pattern. As indicated in the previous sections, multiple factors influence visibility, and the impact of data density may vary with other site characteristics.

3.2 SHAPE METRICS

In addition to the visible point counts, the distribution of those points across each study site was important. Applied to point data, a standard ellipse describes the spatial extent of the points, and can be used to compare spatial distributions among visible points from different scenarios. For this study, a two standard deviation were used to capture 95% of the spatial extent in each of 2 axes. Full parameters (x- and y-axes for each ellipse in each scenario) are provided in Appendix C – Shape Metric Additional Results; representative findings are presented here.

Table 9 shows the length of highest-hit ellipse axes as a percentage of their bare-earth counterparts for Camas NWR. The x- and y-axes do not change consistently, meaning the visible area calculated using a bare-earth DEM cannot be uniformly shrunk to accurately simulate a highest-hit visibility calculation. This is particularly apparent in the 50 m Camas NWR data, where the highest-hit percentage of the bare-earth x-axis length was 93.2%, but the y-axis highest-hit percentage was only 71.1%. Disparity in the x- and y-axis differences between DEM types, for any given structure height, indicates that multiple factors influencing visibility (e.g. topography, asymmetric vegetation, etc.) vary spatially across the site.

The 2 m highest hit x-axis is 100.8% of the bare-earth x-axis, in spite of the visible point count from using the highest-hit DEM being 34.1% lower than the bare-earth visible point count (Table 4). This means that while the maximum extent of points across the landscape is similar between datasets, the concentration of visible points between the lek and the furthest visible point is greater when visibility was calculated using the bare-earth DEM. Thus, to capture two standard deviations of spatial extent, the bare-earth ellipse can actually be narrower than the highest-hit ellipse, which is encircling a more dispersed point set.

Table 9. Two standard deviation ellipse axis parameters for each structure height at the Camas National Wildlife Refuge (NWR) site, from the points visible across either a bare-earth or highest-hit DEM.

Site	Structure Height (m)	Bare-Earth X-axis	Bare-Earth Y-axis	Highest-Hit X-axis	Highest-Hit Y-axis	Highest-Hit X-axis% of Bare-Earth	Highest-Hit Y-axis% of Bare-Earth
Camas NWR	2	2910.2	5292.0	2933.8	4247.9	100.8	80.3
	15	3980.7	6128.1	3391.3	5610.2	85.2	91.6
	50	5581.1	8902.9	5199.4	6333.8	93.2	71.1

Similar results were found for the difference in ellipse shapes among structures, and the amount of change in x- and y-axes differed among 2 m, 15 m, and 50 m structures (Appendix C). For example, the Camas NWR highest-hit, 15 m structure ellipse x-axis was 65.2% of the 50 m structure ellipse x-axis, and the 15 m structure ellipse y-axis was 88.6% of the 50 m structure y-axis. Again, this means that one cannot assume a shorter structure visible area will be some uniform percentage smaller than a taller structure visible area.

4. CONCLUSIONS AND RECOMMENDATIONS

The results presented above serve as a reasonable proof-of-concept to guide future applications of this method. This study shows that using a highest-hit DEM to calculate visibility can, under certain conditions, produce real gains in developable area without exacerbating problematic lek visibility from anthropogenic structures where birds of prey may perch. Additionally, comparisons between datasets of varying point densities provide guidance for future data collection parameters. Each section below contains the conclusions that can be drawn from the study results, and recommendations for possible future implementations.

4.1 SCENARIO APPLICATIONS

Incorporating vegetation into visibility analysis through use of a highest-hit DEM was most impactful on flat or varied terrain, where the topography did not inherently encourage visibility. Little to no effect was seen on terrain that acted as a natural amphitheater. Although vegetation height certainly impacts visibility, it is not a strong predictor *by itself* of potential visibility reductions. Vegetation must be considered in conjunction/coordination/interaction with topography.

Using a highest-hit instead of a bare-earth DEM to calculate visibility does not result in unlimited placement options, anywhere across the landscape, but this study suggests that on suitable sites, 20 – 50% of visible, problematic structure locations can be converted to acceptable, non-visible locations. If substantial variability in visibility reduction between DEM types occurs among structures on a given site, the greatest reduction will likely occur for 2 m structures, and the least reduction for 50 m structures.

The exact visibility reduction is not predictable among structure heights or DEM types. At sites with fairly even vegetation, the visibility reduction associated with using a shorter structure on the bare-earth DEM may be a useful predictor of the visibility reduction associated with that same height structure on the highest-hit DEM, relative to the 50 m structure on each DEM. This could require fewer modeling runs to determine the utility of this technique. At sites with varied vegetation (both height variation and spatial patchiness), the bare-earth structure height related visibility reductions are not good predictors of structure-height related visibility reductions using a highest-hit DEM.

The results also suggest that the spatial extent of the visible area does not change proportionately, either among structure heights on one type of DEM or between bare-earth and highest-hit DEMs for one structure height. Thus, spatial extent findings from one scenario should not be used to predict spatial extents under other scenarios.

The following scenario conditions are most likely to lead to a reduction in structure visibility when using a highest-hit instead of a bare-earth DEM:

- Topography that is not inherently conducive to visibility (e.g. flat or broken, not continuously upward sloping)
- Vegetation of varied heights, not solely taller vegetation
- Shorter structures

4.2 DATA COLLECTION PARAMETERS

Data density is a more important consideration when planning to calculate visibility using a highest-hit DEM instead of a bare-earth DEM.

Using the same point locations, more random points were visible across DEMs derived from the decimated data than DEMs derived from the original data. However, the visible point count difference between the original and thinned data was greater in the highest-hit DEM scenarios than bare-earth DEM scenarios. This was likely due to less accurate capture of the vegetation structure (including the actual shrub height) by the less dense dataset, and similar ground surface accuracies between the two data densities.

The visibility reductions from using the highest-hit instead of bare-earth DEMs were lessened when using the data thinned to a more typical collection standard. This single example does not provide enough information to predict specific reduction percentages associated with specific data densities. However, if a project is a good candidate for calculating visibility using a highest-hit DEM, based on the parameters in Section 4.1, these results do suggest that typical commercial data collection densities (e.g. 4 points/m^2, intermediate between the USGS QL 1 and QL 2 standards) are sufficient to provide real and measurable changes to lek visibility. However, as higher density data becomes available, it should be used in place of lower density data, with an expected, corresponding increased impact on visibility. The maximum point density after which no benefit is gained is unknown.

4.3 MILITARY MISSION BENEFITS

The primary benefit to the military is increasing the land available for development with structures that may serve as perches for predatory raptors without negatively impacting sage-grouse habitat through increased visibility of breeding grounds. This study suggests that on suitable sites, excluded areas can be reduced 20 – 50% by calculating visibility using a highest-hit instead of a bare-earth DEM. This more accurate line-of-sight analysis can allow placement of fences, power poles, towers, or other mission-related structures in areas previously thought unacceptable because of associated raptor activity.

This study directly addressed the 2015 Legacy Area of Emphasis of Readiness and Range Sustainment though mitigation of adverse impacts of natural resources-related encroachment on DoD lands. Reducing the area unavailable for development reduces the encroachment of conservation actions, while still providing for conservation goals. This supports the military's ability to operate in areas within and adjacent to sage-grouse habitat.

In addition to sage-grouse, this approach is also applicable to other species' habitat where visibility is a concern, as well as non-habitat applications. For example, neighboring landowners might be concerned about military construction impacting their viewsheds; this approach could quantify the visibility impact different options for a new structure would have on adjacent lands. Similarly, this approach can also be used in non-ecological applications. As encroachment increases, neighborhood viewsheds will continue to arise as a potential conflict between the military and their civilian neighbors. Across many applications, this approach can guide efforts to maximize site options while minimizing conflicts.

4.4 LESSONS LEARNED

Although these results demonstrate potential visibility reductions from using DEMs created from highest-hit instead of bare-earth LiDAR, this study's approach should be implemented with caution. First, although most LiDAR collection contracts include point classification as a deliverable, if a classified LiDAR dataset (i.e. one with all points classified into at least ground, not-ground, and noise) is not available, this approach is not recommended. Appropriate classification algorithm parameters for the one unclassified dataset used in this study were available from published literature; this is unlikely to be the case for most datasets, and selecting appropriate parameters is a highly technical and potentially time-consuming process.

Table 10. Relationship between point density and nominal point spacing (NPS).

Point Density	NPS
8 pt/m^2	0.354 m
6 pt/m^2	0.408 m
4 pt/m^2	0.500 m
2 pt/m^2	0.707 m
1 pt/m^2	1.0 m
0.25 pt/m^2	2.0 m
0.04 pt/m^2	5.0 m

Second, the minimum spatial resolution of the DEMs is determined from LiDAR data density; creating a 0.5m raster from LiDAR data with 1 pt/m^2 is spatially improper. The analyst creating the DEMs must understand the relationship between point density and raster resolution, and proceed accordingly. The most appropriate relationship between point density and raster resolution depends on the specific application, but in no case should the raster resolution be smaller than the nominal point spacing (NPS). The relationship between nominal point density (NPD) and NPS (assuming an even distribution of points) is calculated as $NPD = 1/NPS^2$ (Heidemann 2014). Typical conversions are shown in Table 10.

If all of the data pre-processing is correctly implemented, the visibility calculations still present a processing challenge, and executing this load solely on a user's primary workstation is not recommended. Although the bare-earth visibility is run using a single ArcGIS tool, it does need to be calculated for each viewer – structure location pair. This proof-of-concept study used 3 points within each lek as viewer locations; in a real-world application, this would likely need to be increased to fully capture the variability within a lek. The highest-hit visibility calculation requires running two tools, doubling the steps for each viewer – structure location pair. Data processing was time consuming, and data organization was critical, although the analysis was completed using standard workstations and software. Use of multiple workstations and virtual machines greatly facilitated data processing for this project.

Although there are many potential challenges, there are also modifications that could increase the feasibility of this type of analysis, and are recommended for future research. First, proposed building sites are usually constrained by a suite of factors applied independent of this analysis (e.g. soil suitability). If a more limited proposed building site delineation were used instead of the entire landscape as a potential site, the number of viewer – structure pairs could be reduced, without reducing the relevant information. This could significantly reduce the workload, while still creating a useful product.

Another modification could be increasing the raster resolution, if larger cell sizes would still adequately capture the vegetation structure. Sage-grouse leks tend to be in sagebrush, which, as a shrub, is best captured with a fine resolution (as demonstrated in this study). However, for other, non-sage-grouse, line-of-site applications in forested areas, a larger cell size might adequately capture canopy structure, and reduce processing demands.

An important caveat to the applicability of these results is that they encompass visibility only. The construction and existence of anthropogenic structures is usually associated with multiple disturbances (e.g., noise, habitat degradation or loss, etc.) that will not be mitigated by revising visibility. These results should be used in conjunction with other ecological and construction considerations to determine the overall impact of a project.

5. APPENDICES

5.1 APPENDIX A – SITE CHARACTERISTICS

Topographic variation among sites is shown in Figure 6. Each elevation profile is outward from the lek, across the width of the analysis area. This illustrates the topological differences among sites: Borah Scarp (shown in green) is a generally continuous rise from the lek, Reynolds Creek (shown in orange) has varied terrain before a significant elevation gain, and Camas NWR (shown in blue) has little elevation change. Bearings for each transect profile are given in Table 11.

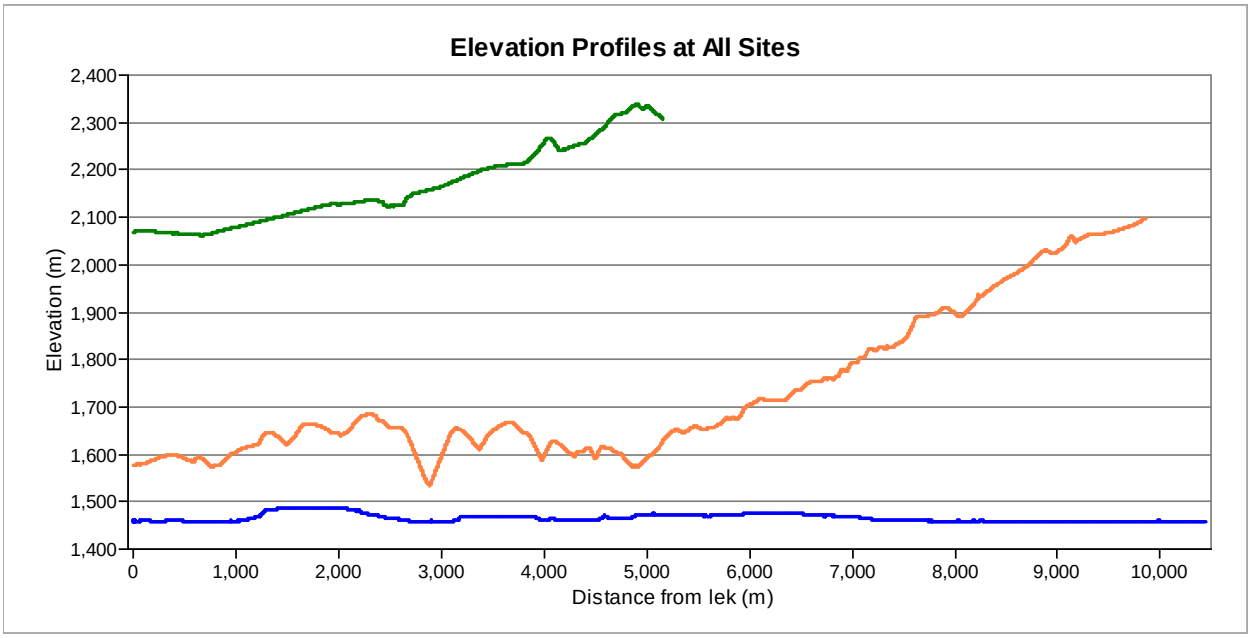

Figure 6. Elevation transect profiles for Borah Scarp (green), Reynolds Creek (Orange), and Camas NWR (blue). Each profile extends from the lek at distance 0 across the analysis area. Note that the Borah Scarp profile is a shorter distance because the analysis area was smaller than the other sites.

Variation in vegetation height (the difference between the highest-hit and bare-earth DEMs) is shown in Figure 7. Each vegetation profile follows the same line as the elevation profile in Figure 6. The first 5000 m away from the lek is illustrated, as that distance is common to all sites. The Reynolds Creek transect profile, shown in orange, encounters more vegetation that reaches taller heights than either Borah Scarp (shown in green) or Camas NWR (shown in blue). Bearings for each transect profile are given in Table 11.

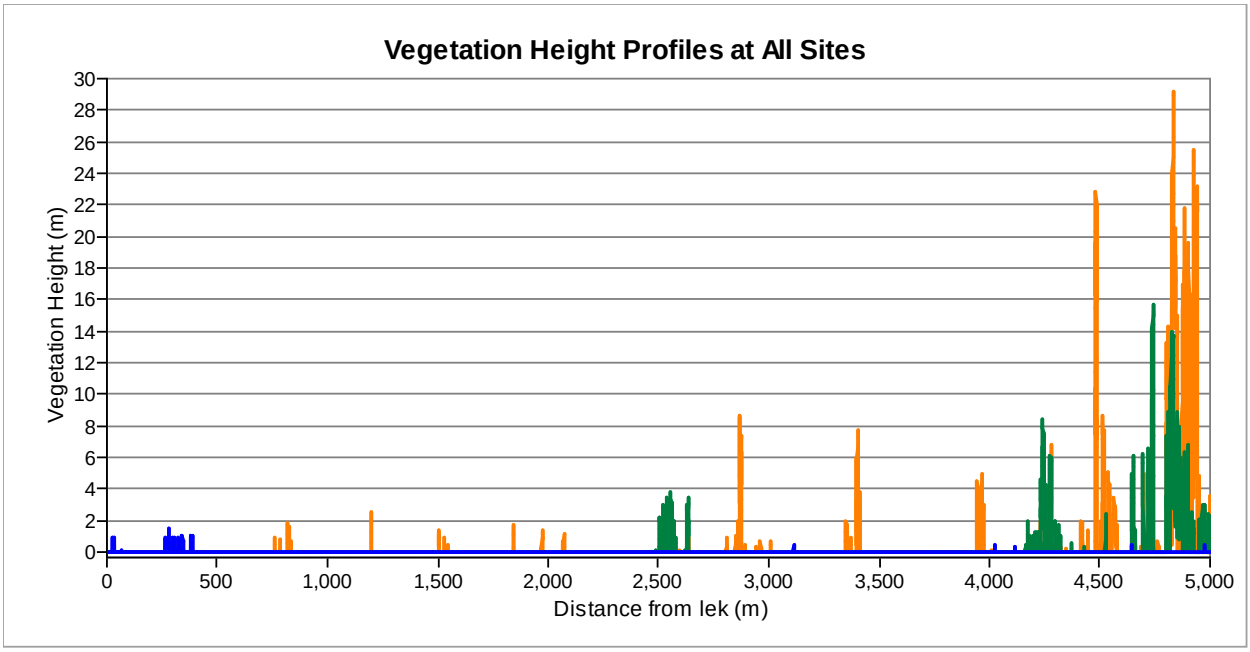

Figure 7. Vegetation transect profiles for Borah Scarp (green), Reynolds Creek (Orange), and Camas NWR (blue). Each profile extends from the lek at distance 0 across the first 5000 meters of the analysis area.

Table 11. Bearing from lek used for elevation and vegetation transects.

Site	Transect Bearing from Lek (degrees)
Borah Scarp	146
Camas NWR	279
Reynolds Creek	219

5.2 APPENDIX B – RASTER GENERATION PARAMETERS

Table 12. Raster creation settings. Not all classes were present in all datasets. Note that the data report for Camas NWR specifies that Class 4, which is typically Medium Vegetation, was used for road surfaces in that dataset.

ArcGIS 10.2 Raster Creation				
Site	**Raster Type**	**.LAS Classes Used**	**Cell Assignment**	**Cell Size**
Borah Scarp	Bare-earth	2	Average	0.5 m
	Highest-hit	1, 2, 3, 4, 8, 9	Maximum	0.5 m
Camas NWR	Bare-earth	2, 4, 9	Average	0.3048 m (~ 1 ft.)
	Highest-hit	1, 2, 3, 4, 5, 9, 10	Maximum	0.3048 m (~ 1 ft.)
Camas NWR decimated	Bare-earth	2, 4, 9	Average	1 m
	Highest-hit	1, 2, 3, 4, 5, 9, 10	Maximum	1 m
Reynolds Creek	Highest-hit	1, 2, 3	Maximum	0.5 m
BCAL LiDAR Tools Raster Creation				
Site	**Raster Type**	**Tool**	**Settings**	**Cell Size**
Reynolds Creek	Bare-earth	Buffer .LAS Files	20 m	n/a

		Perform Height Filtering	7m Canopy Spacing 0.1 Threshold	n/a
		Create Bare-earth DEM	n/a	0.5 m

5.3 APPENDIX C – SHAPE METRIC ADDITIONAL RESULTS

The tables below contain the complete parameters of two standard deviation ellipses for each scenario.

Table 13. Two standard deviation ellipse axis parameters for each structure height at each of three study sites, from the points visible across either a bare-earth or highest-hit DEM. The highest-hit X- and Y-axes are also calculated as percentages of their respective bare-earth axes.

Site	Structure Height (m)	Bare-Earth X-axis	Bare-Earth Y-axis	Highest-Hit X-axis	Highest-Hit Y-axis	Highest-Hit X-axis% of Bare-Earth	Highest-Hit Y-axis% of Bare-Earth
Borah Scarp	2	2094.5	4051.9	2099.5	3818.6	100.2	94.2
	15	2305.1	4084.6	2297.0	4075.5	99.6	99.8
	50	2502.9	4126.5	2502.9	4123.9	100.0	99.9
Camas NWR	2	2910.2	5292.0	2933.8	4247.9	100.8	80.3
	15	3980.7	6128.1	3391.3	5610.2	85.2	91.6
	50	5581.1	8902.9	5199.4	6333.8	93.2	71.1
Reynolds Creek	2	2544.4	8034.9	2260.3	7529.7	88.8	93.7
	15	2813.6	8197.8	2491.4	7944.9	88.5	96.9
	50	3329.0	8783.2	3213.6	8688.4	96.5	98.9

Table 14. Two standard deviation ellipse axis parameters for each structure height at each of three study sites, from the points visible across either a bare-earth or highest-hit DEM. The bare-earth and highest-hit X- and Y-axes are also calculated as percentages of their respective maximum extents.

Site	Structure Height (m)	Bare-Earth X-axis	Bare-Earth Y-axis	% Max Bare-Earth X-axis	% Max Bare-Earth Y-axis	Highest-Hit X-axis	Highest-Hit Y-axis	% Max Highest-Hit X-axis	% Max Highest-Hit Y-axis
Borah Scarp	2	2094.5	4051.9	83.7	98.2	2099.5	3818.6	83.9	92.6
	15	2305.1	4084.6	92.1	99.0	2297.0	4075.5	91.8	98.8
	50	2502.9	4126.5	100.0	100.0	2502.9	4123.9	100.0	100.0
Camas NWR	2	2910.2	5292.0	52.1	59.4	2933.8	4247.9	56.4	67.1
	15	3980.7	6128.1	71.3	68.8	3391.3	5610.2	65.2	88.6
	50	5581.1	8902.9	100.0	100.0	5199.4	6333.8	100.0	100.0
Reynolds Creek	2	2544.4	8034.9	76.4	91.5	2260.3	7529.7	70.3	86.7
	15	2813.6	8197.8	84.5	93.3	2491.4	7944.9	77.5	91.4
	50	3329.0	8783.2	100.0	100.0	3213.6	8688.4	100.0	100.0

Table 15. Two standard deviation ellipse axis parameters for each structure height at each data density, from the points visible across either a bare-earth or highest-hit DEM using the original and decimated Camas NWR data. The highest-hit X- and Y-axes are also calculated as percentages of their respective bare-earth axes.

Site	Structure Height (m)	Bare-Earth X-axis	Bare-Earth Y-axis	Highest-Hit X-axis	Highest-Hit Y-axis	Highest-Hit X-axis% of Bare-Earth	Highest-Hit Y-axis% of Bare-Earth
Camas NWR	2	2910.2	5292.0	2933.8	4247.9	100.8	80.3
	15	3980.7	6128.1	3391.3	5610.2	85.2	91.6
	50	5581.1	8902.9	5199.4	6333.8	93.2	71.1
Camas NWR Decimated	2	2935.6	5386.8	2942.7	4232.9	100.2	78.6
	15	4071.0	6133.1	3401.0	5603.6	83.5	91.4
	50	5493.4	9430.9	5302.7	6328.2	96.5	67.1

Table 16. Two standard deviation ellipse axis parameters for each structure height at each data density, from the points visible across either a bare-earth or highest-hit DEM, using the original and decimated Camas NWR LiDAR datasets. The bare-earth and highest-hit X- and Y-axes are also calculated as percentages of their respective maximum extents.

Site	Structure Height (m)	Bare-Earth X-axis	Bare-Earth Y-axis	% Max Bare-Earth X-axis	% Max Bare-Earth Y-axis	Highest-Hit X-axis	Highest-Hit Y-axis	% Max Highest-Hit X-axis	% Max Highest-Hit Y-axis
Camas NWR	2	2910.2	5292.0	52.1	59.4	2933.8	4247.9	56.4	67.1
	15	3980.7	6128.1	71.3	68.8	3391.3	5610.2	65.2	88.6
	50	5581.1	8902.9	100.0	100.0	5199.4	6333.8	100.0	100.0
Camas NWR Decimated	2	2935.6	5386.8	53.4	57.1	2942.7	4232.9	55.5	66.9
	15	4071.0	6133.1	74.1	65.0	3401.0	5603.6	64.1	88.6
	50	5493.4	9430.9	100.0	100.0	5302.7	6328.2	100.0	100.0

6. ACKNOWLEDGEMENTS

This project was fully funded by the Department of Defense Legacy Resource Management Program as project number 15-800, through agreement number HQ0034-15-2-0009.

Michelle Commons-Kemner, Curtis Hendricks, and Bartholomew Zwetzig provided detailed lek locations.

Dr. Nancy Glenn, University of Idaho, provided assistance with BCAL LiDAR Tools.

Amy Burzynski assisted with shape metric data processing and document revision.

7. REFERENCES

BCAL Lidar Tools ver 2-dev 11. Boise State University, Department of Geosciences, 1910 University Drive, Boise, Idaho. URL: http://bcal.boisestate.edu/tools/lidar

Braun, C.E., Oedekoven, O.O., and C.L. Aldridge. 2002. Oil and gas development in western North America: effects on sagebrush steppe avifauna with particular emphasis on sage-grouse. *Transactions of the North American Wildlife and Natural Resources Conference*, 67: 337-349.

Connelly, J.W., S.T. Knick, M.A. Schroeder, and S.J. Stiver. 2004. *Conservation Assessment of Greater Sage-grouse and Sagebrush Habitats.* Western Association of Fish and Wildlife Agencies. Unpublished Report. Cheyenne, WY. Available at https://sagemap.wr.usgs.gov/docs/Greater_Sage-grouse_Conservation_Assessment_060404.pdf.

ESRI. 2013. ArcGIS Desktop: Release 10.2. Redlands, CA: Environmental Systems Research Institute.

Farmer, P. and Beaver, J. 2010. *An Approach for Implementing Mitigation Measures to Minimize the Effects of Construction and Operation of the Keystone XL Pipeline Project on Greater Sage-Grouse.* WESTECH Environmental Services, Inc. Helena, MT. Available at https://keystonepipeline-xl.state.gov/documents/organization/182249.pdf

Greater Sage-Grouse Habitat Conservation Strategy for NRCS in Idaho. n.d. Available at https://www.nrcs.usda.gov/Internet/FSE_DOCUMENTS/nrcs144p2_041631.pdf

Heidemann, H. K. 2014. *LiDAR base specification (ver. 1.2, November 2014): U.S. Geologic Survey Techniques and Methods*, Book 11, Chapter B4, 67p. Available at http://dx.doi.org/10.3133/tm11B4

Hovick, T. J., Elmore, R. D., Dahlgren, D. K., Fuhlendorf, S. D. and Engle, D. M. 2014. REVIEW: Evidence of negative effects of anthropogenic structures on wildlife: a review of grouse survival and behaviour. *Journal of Applied Ecology*, 51: 1680–1689. DOI: 10.1111/1365-2664.12331

Idaho Sage-grouse Advisory Committee, Technical Assistance Team. 2016. *Idaho Sage-grouse Local Working Groups Statewide Annual Report 2015*. Available at https://docs.google.com/viewer?url=https%3A%2F%2Fidfg.idaho.gov%2Fsites%2Fdefault%2Ffiles%2Flwg-annual-report-2015.pdf

Magnusson, M., Fransson, J.E.S., and Holmgren, J. 2007. Effects on estimation accuracy of forest variables using different pulse density of laser data. *Forest Science*, 53 (6): 619-626. ISSN 0015-749X.

MassGIS. 2017. *MassGIS Data – LiDAR Terrain Data*. Available at http://www.mass.gov/anf/research-and-tech/it-serv-and-support/application-serv/office-of-geographic-information-massgis/datalayers/lidar.html

Mitchell, J. J., Glenn, N. F., Sankey, T. T., Derryberry, D. R., Anderson, M. O., and Hruska, R. C. 2011. Small-footprint LiDAR estimations of sagebrush canopy characteristics. *Photogrammetric Engineering and Remote Sensing*, 77 (5): 521-530. DOI: 10.14358/PERS.77.5.521

Oregon LiDAR Consortium. n.d. *Exhibit A to Amendment 5 to Agreement #8865, Description and Specification of the Services*. Available at http://www.oregongeology.org/sub/projects/olc/olc_lidar_spec.pdf

Puget Sound LiDAR Consortium. n.d. *A. Technical Specifications*. Available at http://pugetsoundlidar.ess.washington.edu/Technical_Specifications_withAppendices.pdf

Roberson, E. L. 2009. *Managing Structures for the Safety of Sage-grouse, Sharp-tailed grouse, and Lesser Prairie-chicken* [Memorandum]. Washington, DC: U.S. Department of the Interior, Bureau of Land Management. Available at https://www.blm.gov/policy/im-2010-022-0

Streutker, D. and N. Glenn. 2006. LiDAR measurement of sagebrush steppe vegetation heights. *Remote Sensing of Environment*, 102: 135-145. DOI: 10.1016/j.rse.2006.02.011

U.S. Department of the Interior, Bureau of Land Management, Idaho State Office. 2015. *Greater Sage-Grouse Habitat Management Areas of the Great Basin Region, Idaho-SW Montana Sub-region, Greater Sage-grouse Environmental Impact Statement (EIS) - Administrative Draft Proposed Plan, as updated for inclusion of Sagebrush Focal Areas.* Vector digital data. Available at http://cloud.insideidaho.org/webApps/metadataViewer/default.aspx?path=%5c%5cintranet.rocket.net%5cinsideprod%5cdata%5canonymous%5cblm%5cGRSG_FINALEIS_ID_Habitat_ProposedPlan.shp.xml

Vierling, L., Xu, Y., Eitel, J.U.H., and J. Oldow. 2012. Shrub characterization using terrestrial laser scanning and implications for airborne LiDAR assessment. *Canadian Journal of Remote Sensing*, 38 (6): 790-722.

Walker, B. L., Naugle, D. E., and Doherty, K. E. 2007. Greater sage-grouse population response to energy development and habitat loss. *Journal of Wildlife Management*, 71:2644-2654.